Physical Characterization of Layered Perovskites–Polystyrene Composites

VINCENZO BUSICO and PAOLO CORRADINI, *Istituto Chimico dell'Università, Naples,* CLAUDIO MIGLIARESI* and LUIGI NICOLAIS, *Istituto di Principi di Ingegneria Chimica Facoltà di Ingegneria, 80125 Naples, Italy*

Synopsis

Mechanical and thermal properties of layered perovskites–polystyrene composites have been studied over a wide range of temperature and filler content. The layered perovskites show a solid–solid transition at a temperature which is dependent on the number of the carbon atoms in the hydrocarbon chains and on the nature of the metal atom. The system PS–C_{12} Mn shows relatively good mechanical properties even at high filler content. These properties, coupled with an excellent thermal behavior of the "thermally active" filler inside the polymeric matrix, make the title composites of interest in the field of thermal-energy storage.

INTRODUCTION

In recent years, an increasing number of articles have been published concerning particulate-filled plastic materials and their physical properties. In particular, the mechanical behavior of plastic materials reinforced by rigid fillers has been the main subject of study, and recent reviews[1,2] give a good indication of the parameters controlling the mechanical behavior of such materials.

The present article deals with composites characterized by a filler showing poor mechanical properties, but a peculiar thermal behavior which makes it of potential interest in the field of thermal-energy storage systems.

In these composites with "thermally active" fillers, a polymeric matrix has been used to give the incoherent filler mechanical properties allowing both the static lift and the straightforward and cheap processing of the resulting material.

LAYERED PEROVSKITES AND THEIR POLYSTYRENE COMPOSITES

The composites are composed of a polystyrene matrix filled with an organometallic compound of formula

$$(n\text{-}C_{12}H_{25}NH_3)_2\ MnCl_4$$

In the last few years, several articles[3–10] have been published on compounds of general formula $(n\text{-}C_nH_{2n+1}NH_3)_2\ MCl_4$, where M is a divalent metal atom and $8 \leq n \leq 18$. These compounds have been given the inclusive denomination of "layer perovskites" because for M = Mn(II)[3(a),3(b)], Cu(II)[4–5], Hg(II)[6], Cd(II), and Fe(II)[7–8], their structure resembles that of the mineral perovskite, $CaTiO_3$, and results from the regular alternation of inorganic and hydrocarbon regions,

Journal of Applied Polymer Science, Vol. 25, 2857–2868 (1980)

0021–8995/80/0025–2857$01.20

so that each inorganic layer is sandwiched between two hydrocarbon layers, and vice versa [Fig. 1(a)].

In the compounds with M = Mn(II)[3(a),3(b)], the inorganic layers consist of nearly two-dimensional macroanions, made up of octaedral $MnCl_6$ units sharing corners [Fig. 1(b)]. As it results from the general formula, the hydrocarbon regions are formed by the linear alkyl chains of the alkylammonium groups, which take on a double-layer chain packing, without intercalation of chains from adjacent layers. The chains are inclined, with respect to the perpendicular of the inorganic layers, of an angle which has been calculated from x-ray observations to be about 45°. The overall structure results from the piling up of "sandwiches" of composition $(n\text{-}C_nH_{2n+1}NH_3)_2\,MnCl_4$; between two successive sandwiches the binding forces are of the Van der Waals type among the methyl ends of the chains [Fig. 1(a)].

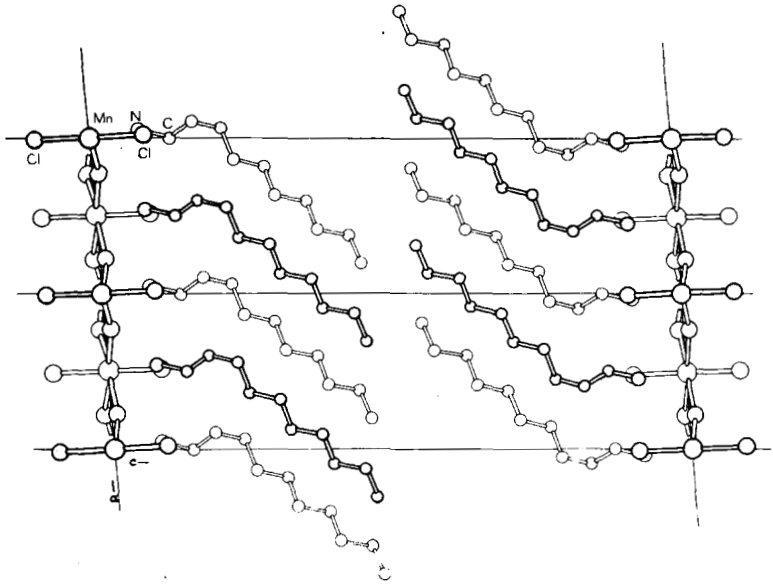

(a)

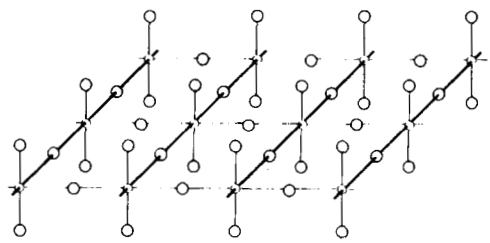

(b)

Fig. 1. (a) Mode of packing of the alkyl chains in the ordered polymorphs of the layer perovskites: compound $(n\text{-}C_{10}H_{21}NH_3)_2\,MnCl_4$.[11] (b) Schematic view of a portion of the macroanion in the layer perovskites with M = Mn(II)[11], showing the coordination of the metal atom. The larger circles represent chlorine atoms. (O) Mn(II), (◯) Cl.

The thermal behavior of the layered perovskites, in general, and of those with M = Mn (II) in particular, is characterized by high-enthalpy reversible solid–solid phase transitions between two polymorph forms, in the temperature range 273–373 K. These transitions have been proven[9–10] to be of the order–disorder kind, and to involve only the hydrocarbon parts of the structure. In more detail, in the lower temperature-stable forms of the layered perovskites, the long chains of the alkylammonium groups are conformationally ordered, with all their carbon–carbon skeletal bonds in a trans state (except one bond, usually between the C_2 and C_3, which is in a gauche state, allowing the chains to be inclined as previously described). On the other hand, in the higher temperature-stable polymorphs the alkyl chains take on a disordered arrangement, and gain a conformational freedom comparable with what they would have in the melt. In other words, in these polymorphs, although their overall structure remains solid, the hydrocarbon regions are in a liquidlike state.[9–11]

The transition parameters of the layered perovskites are strongly dependent on the number of the carbon atoms of the hydrocarbon chains and on the nature of the metal atom.

Even if the alkyl chains in the hydrocarbon regions are fixed at one end and the volume available to them is limited, the transition enthalpies per mole of alkyl chain in the layered perovskites are not much lower than the molar melting enthalpies of the corresponding normal paraffins (of course, the total transition enthalpies are lower, because they take into account the weight of the inorganic regions, which are inert since they do not contribute to the transitions).

Therefore, as the *n*-paraffins, the layered perovskites are candidate systems for latent heat thermal-energy storage; as compared to the former, they have the advantage of remaining solid after the transition. On the other hand, although the thermal behavior of the layered perovskites is quite satisfactory, their mechanical properties are very poor. In order to obtain self-carrying materials for large-scale thermal experiments, we have prepared composites composed of a polymeric matrix filled with various layered perovskites.

In the present article, we refer to the preparation and some physical properties of composites composed of $(n\text{-}C_{12}H_{25}NH_3)_2\ MnCl_4$–polystyrene (in the following, they will be indicated as PS–C_{12}Mn). The transition parameters of C_{12}Mn as calculated from DSC scans, at a scanning rate of 10 K/min, are:

Transition temperature

$$T_{tr} = \begin{cases} 332\text{ K (heating scans)} \\ 320\text{ K (cooling scans)} \end{cases}$$

Transition enthalpy

$$\Delta H_{tr} = 19\text{ cal/g}$$

These parameters remain unaltered even after numerous thermal cycles through the transition points.

EXPERIMENTAL

The composites PS–C_{12}Mn were prepared by conventional compression molding techniques. The appropriate volumes of injection-molding-type powders of polystyrene (Montedison Edistir FA, with an average particle size

of the order of 170 μm) and of the finely powdered layered perovskite $C_{12}Mn$ (average particle size 150 μm) were extensively dry blended at room temperature.

The mixtures were placed in a compression mold at the temperature of 130°C and a pressure of 50 kg/cm^2 for 15 min to produce smooth, flat slabs 14.0 × 7.0 × 0.5 cm, or strips 14.0 × 1.5 × 0.3 cm containing 20, 40, 50, 60, 70, and 80% $C_{12}Mn$ (the densities of the two component phases can be considered the same, both being about 1.1 g/cm^3. This means that the volume and weight fractions are identical).

Tensile and flexural (three-point bending[12]) stress–strain tests on the composite strips were carried out using an Instron 1112 testing machine equipped with a thermostatically controlled oven. The tests were conducted at a constant rate of deformation of 0.5 cm/min, utilizing a gauge length of 5 cm in the tensile tests and 10 cm in the flexural ones.

The tensile tests were performed at 20°C only, the flexural measurements at 20, 40, 60°C.

The apparent modulus or rigidity in torsion, G, of all the materials was measured using a Clash–Berg torsion stiffness tester. Temperature was controlled by immersion of the sample in a Dewar flask containing a silicone fluid. The tests were performed at variable temperature between 0 and 100°C.

Microsamples of the composites PS–$C_{12}Mn$ at various filler content were subjected to differential thermal analysis, utilizing a differential thermal calorimeter Perkin–Elmer DSC-2.

The thermograms were registered between 0 and 100°C, at a scanning rate of 10 K/min, in a running N_2 atmosphere. The transition enthalpies were calculated using as a standard a sample of pure indium (ΔH_m = 28.5 J/g).

Thermal conductivity data at room temperature were obtained on a thermoconductometer Colora (the two liquids utilized were diethylether and carbon disulfide).

Finally, the composite slabs were utilized for insulation tests; these were performed by placing one major face of a slab on a hot plate previously thermostatted at a given exercise temperature $T_e > T_{room}$ and following the temperature variation with time at the opposite face of the slab by means of a thermocouple stuck on this cold face.

Micrographs of the fracture surfaces of several composite strips subjected to tensile stress–strain tests were obtained using a Cambridge scanning electron microscope.

RESULTS AND DISCUSSION

Thermal Behavior

The differential calorimetric analysis of the composites under examination shows that the compound $(n\text{-}C_{12}H_{25}NH_3)_2\ MnCl_4$ keeps its thermal behavior and parameters (see Layered Perovskites Section) unaltered even when it is included in the polymeric matrix.

The importance of this conclusion is self-evident in utilizing, as in this case, the title composites in the field of thermal-energy storage.

On the other hand, the insulating properties of the materials under study are emphasized by the results of the insulation tests described in the previous section. Typical curves—temperature of the cold face vs. time, for the composite PS–$C_{12}Mn$ with a filler content of 60%—are reported in Figure 2, for various testing temperatures of the thermostatted hot plate (and hence, of the hot face). All the curves show a more or less wide plateau at a temperature near the transition of the filler.

In Figure 3, we report the width of the plateau as a function of the filler content, relative to tests performed at various temperatures of the hot plate.

From Figures 2 and 3 it can be inferred that the less the difference between the hot plate temperature and the transition temperature, the more effective the insulation effect, and that the greatest insulation is the composite with a filler content of about 60%, which corresponds roughly to the maximum filler loading without contact of the particles constituting the dispersed phase.

Accordingly, from Figure 4 it can be seen that the thermal conductivity λ is quite constant for composites with a filler fraction of between 0 and 60%. Inside this range, an increment of filler content results in an increased thermal capacity of the composite, at constant λ, hence in a wider plateau and a more effective insulation. When the filler fraction exceeds 60%, the thermal capacity of the samples keeps on growing, but it effects the necklace formation of the filler, so that the heat transfer happens preferentially through the particles of the dispersed phase (this results in an increase of λ).

Of these two opposite effects, it is the latter which is of the greatest importance, so that the insulating properties of the composites are reduced.

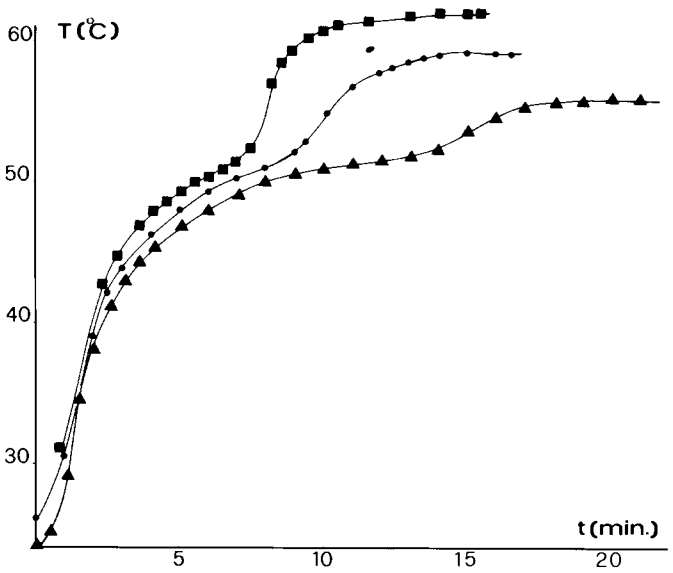

Fig. 2. Time dependence of the temperature of the cold surface of a 0.5-cm thick composite slab with a filler content $\phi = 0.6$, heated at 65°C (▲), 70°C (●), and 75°C (■) from the opposite surface.

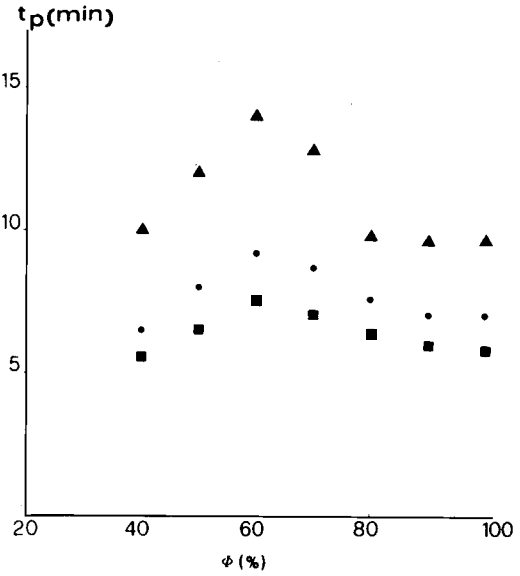

Fig. 3. Duration of the plateau effect, t_p, vs. filler content, ϕ, for several 0.5-cm thick composite slabs heated at 65°C (▲), 70°C (●), 75°C (■).

Mechanical Behavior

In Figure 5 the shear modulus G for pure PS and a typical composite PS–C_{12}Mn (filler fraction 40%) is reported as a function of temperature. It is possible to verify that the inclusion of the salt C_{12}Mn into the polymeric matrix does not change the T_g of PS, and, in agreement with the calorimetric data, the thermal behavior of the filler is not altered after the inclusion into the matrix. Moreover, the shear modulus of the composite is, at temperatures $T < T_{tr}$, constantly below that of pure PS, showing that the shear modulus of the filler is smaller than that of unfilled PS. Once the temperature reaches T_{tr}, a new decrease in the shear

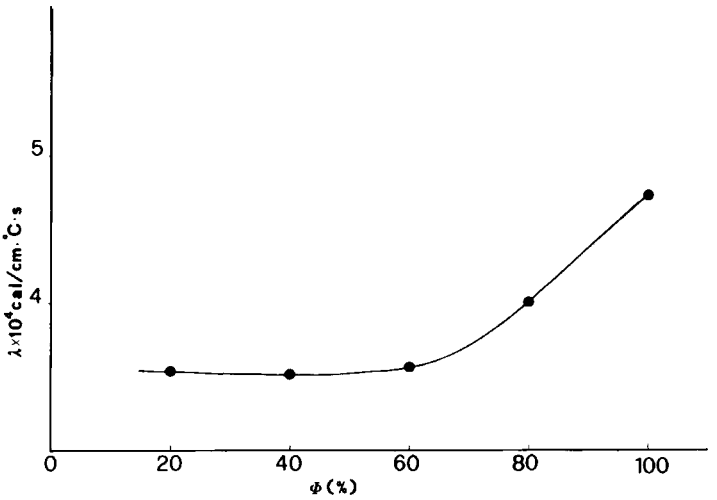

Fig. 4. Room temperature thermal conductivity, λ, of composites PS–C_{12}Mn vs. their filler content, ϕ.

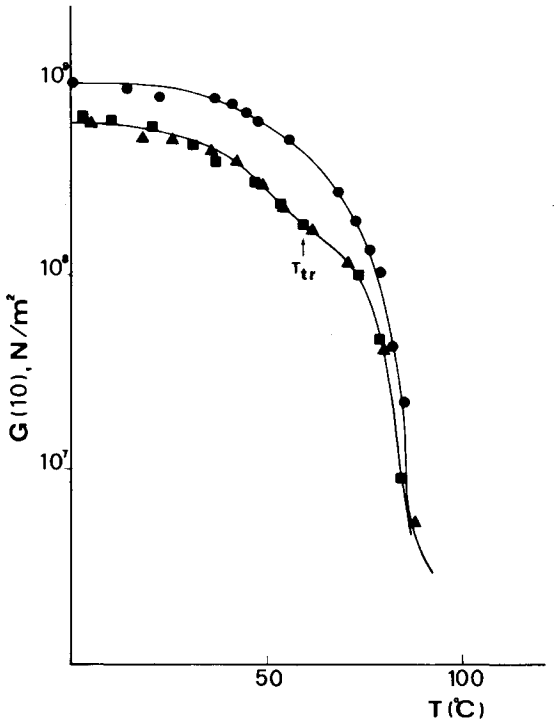

Fig. 5. Apparent modulus of rigidity in torsion G for pure PS (●) and the composite PS–$C_{12}Mn$ with a filler content $\phi = 0.4$ (▲, ■) as a function of temperature. T_{tr} = transition temperature of the filler.

modulus of the composite occurs, indicating a further reduction of the modulus of $C_{12}Mn$. This effect could have been expected, since the phase transition implies the change of the filler to a disordered form, with the consequent reduction of its rigidity.

Figure 6 shows typical tensile stress–strain curves obtained from tests performed at room temperature on pure PS and on PS–$C_{12}Mn$ composites at various filler content. With increasing filler fraction, there is a decrease of the Young moduli and of the strength of the systems, while the ultimate elongation, after an increase for $\phi = 0.2$, decreases progressively.

Similar data have also been obtained in flexure using a three-point bending[12] device.

In Figure 7 the room temperature tensile and flexural moduli (relative to those of pure PS) E_r of the title composites versus their filler content are plotted. While the flexural elastic modulus decreases very smoothly with increasing filler concentration, and remains of the same order of magnitude as that of pure PS, even when the filler fraction reaches 80%, the tensile elastic modulus drops quickly with increasing filler content.

This disparity in the trend of the two different kinds of elastic moduli can be explained on the grounds of the microscopic structure of the filler.

In fact, as we have previously said, the layered perovskite $C_{12}Mn$ is a typical sandwich compound, constituted by the piling of successive two-dimensional layers—inside which covalent forces predominate—upon the third axis, per-

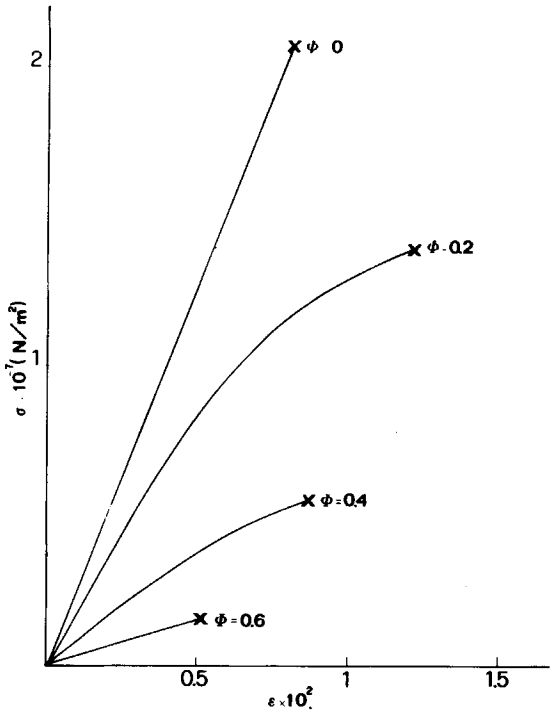

Fig. 6. Typical tensile stress–strain curves at room temperature for pure PS and several PS–$C_{12}Mn$ composites.

pendicular to these layers. The forces assembling the overall structure are just weak forces of the Van der Waals type [Fig. 1(a)]. Consequently, it is intuitive that the mechanical behavior of a single crystal of this compound will be markedly anisotropic since it will be characterized by a relatively good resistance to the stresses directed perpendicularly to the two-dimensional layers and a great flakiness (in consequence of stresses directed tangentially to the layers).

The macroscopic appearance of the crystals of $C_{12}Mn$ is strongly influenced

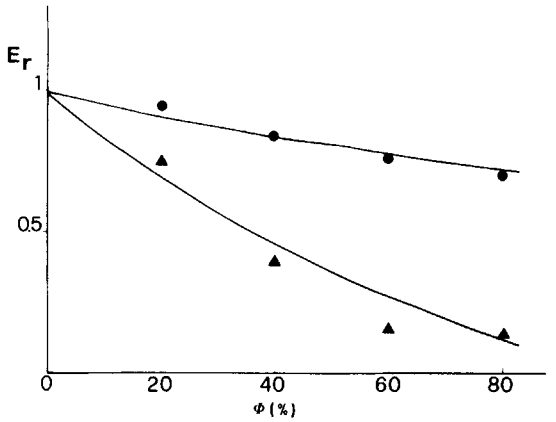

Fig. 7. Room-temperature tensile (▲) and flexural (●) elastic moduli (relative to those of pure PS), E_r, of the title composites vs. their filler content, ϕ. The continuous curves plot the theoretical values of E_r vs. ϕ, calculated on the ground of Kerner eq. (1).

by its microscopic structure. In fact, the crystals are typical plateletlike ones, with their thicknesses greatly reduced when compared with the remaining two dimensions, even after prolonged grinding. Consequently, the crystallites in the powder of $C_{12}Mn$ do not orient themselves statically but take on a preferential common orientation, with the two-dimensional layers parallel to the surface of the sample holder. This can be evidenced by the x-ray powder spectra of the compound, characterized by a series of reflection maxima from planes parallel to the layers [(001) reflections] that are integral multiples of a unique interlayer spacing, corresponding to the distance between two successive inorganic regions in the structure[3(a),3(b)] (in the specific case of C_{12} Mn, 30.28Å).

The only difference after the transition is the increment of this distance (for C_{12} Mn from 30.28 to 33.41 Å) owing to the larger volume occupied by the hydrocarbon chains in their disordered arrangement.

As happens in the powders, the orientation of the filler particles in the polymeric matrix, too, is not random; they tend to orient themselves with their two-dimensional layers parallel to the major surfaces of the samples. This is at the origin of the different mechanical behavior of the title composites in tension and in flexure. In fact, in the flexural stress–strain tests, the applied stresses are perpendicular to the major surfaces of the samples and, hence, to the two-dimensional layers of the filler, a direction in which this presents its higher modulus. In the tensile tests, on the other hand, the applied stresses are tangential to the layers, a direction in which the modulus of the filler is poor.

The good adhesion between the two phases (evidenced by the trend of the flexural modulus) is confirmed by the micrographs of the fracture surfaces of samples subjected to stress–strain tests [Figs. 8(a)–8(c)]. In fact, it is not possible to distinguish between the component phases, since the materials look extremely compact and homogeneous, or to recognize the typical "craters," because of the expulsion of particles of filler, peculiar to compounds characterized by a poor adhesion between the filler and the matrix.[1]

A semiquantitative interpretation of the data shown in Figure 7 has been attempted by calculating the theoretical trend of the elastic moduli of the title composites versus their filler content on the ground of the Kerner equation[1]:

$$\frac{E_c}{E_p} = E_r = \frac{1 + AB\,\phi}{1 - B\,\phi} \tag{1}$$

for

$$A = \frac{7 - 5\nu}{8 - 10\nu}$$

$$B = \frac{(E_2/E_p) - 1}{(E_2/E_p) + A}$$

ν = Poisson ratio = 0.33

ϕ = filler concentration

E_2 = elastic modulus of the filler

E_p = elastic modulus of the polymer

E_c = elastic modulus of the composite.

The values of E_2 were obtained by extrapolating to $\phi = 1$ the experimental data from stress–strain tests (performed for $0 \leq \phi \leq 0.8$).

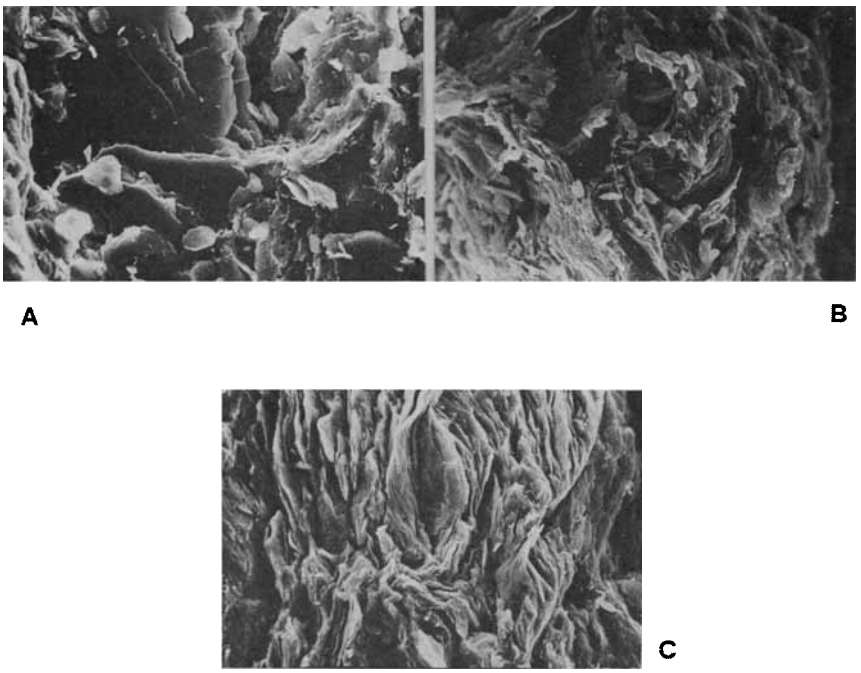

Fig. 8. Micrographs of the fracture surfaces of samples of composites PS–C_{12}Mn at various filler concentrations, ϕ, subjected to tensile stress–strain tests: (a) $\phi = 0.2$, 500×; (b) $\phi = 0.5$, 500×; (c) $\phi = 0.8$, 500×.

The calculated values of E_2 are diagrammed in Figure 7 (continuous curves). The agreement with the experimental data is quite satisfactory, confirming the possibility of calculating by extrapolation the elastic moduli of an incoherent substance by its inclusion into a polymeric matrix, in case of adhesion between the two phases.

The same treatment was operated on the experimental data relative to the flexural elastic moduli at variable temperature (20, 40, and 60°C, Fig. 9). The

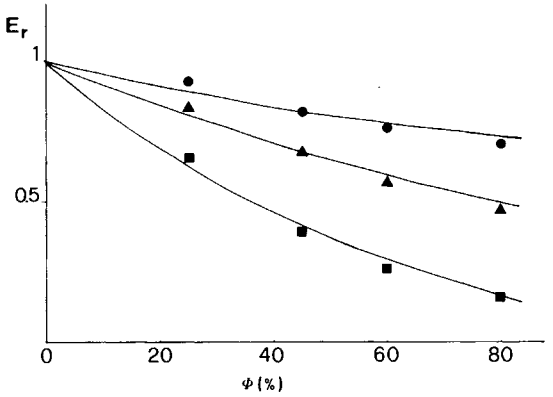

Fig. 9. Flexural elastic moduli of the title composites (relative to those pure PS), E_r, vs. their filler concentration ϕ at variable temperature (● 20°C, ▲ 40°C, ■ 60°C). The continuous curves plot the theoretical values of E_r vs. ϕ, calculated on the ground of the Kerner eq. (1).

agreement of these data with the theoretical Kerner curves calculated from eq. (1) is still very good. The drop of the moduli of the title composites when the filler is in its disordered form (T = 60°C) can be interpreted by assuming that the modulus of the filler decreases sharply after the transition. Even, in this case the composite materials remain self-carrying.

Finally, in Figure 10 the ultimate tensile and flexural stresses of the PS–$C_{12}Mn$ composites (relative to those of pure PS) σ_{br} versus filler content are reported and compared with the theoretical trend calculated from the equation of Nicolais and Narkis[13]:

$$\sigma_{br} = \frac{\sigma_c}{\sigma_p} = 1\text{–}1.21\ \phi^{2/3} \tag{2}$$

obtained in the hypothesis of no adhesion between filler and matrix, and that the applied load is supported only by the matrix.

The agreement between the experimental and the theoretical ultimate tensile stresses is due to the peculiar structural anisotropy of the composites under study rather than to poor adhesion between the two phases.

In conclusion, the comprehensive mechanical behavior of the PS–$C_{12}Mn$ composites can be considered quite satisfactory, since they show relatively high-flexural elastic moduli, and even in tension they are always fully self-carrying. Both these encouraging mechanical properties and the optimal thermal behavior of the thermally active filler inside the polymeric matrix make the title composites of interest in the field of thermal-energy storage by means of systems undergoing primary phase changes within the range of operation.[14]

On the other hand, the successful semiquantitative analysis conducted in this section confirms that in the case of adhesion between the two phases, it is possible to evaluate the mechanical parameters of an incoherent substance by including it in a polymeric matrix and extrapolating the properties of the resulting composite materials through theoretical equations from the literature.

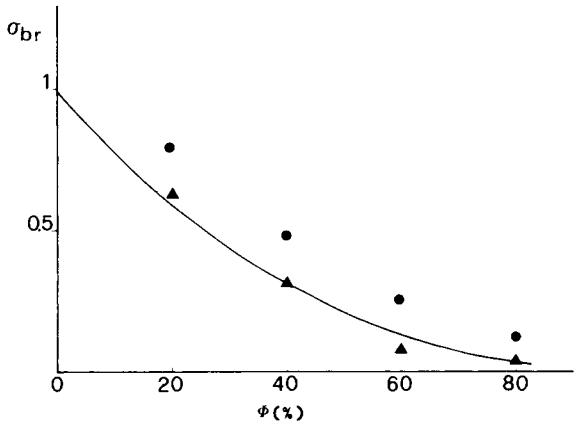

Fig. 10. Ultimate tensile (●) and flexural (▲) stresses (relative to those of pure PS) σ_{br} of the composites PS–$C_{12}Mn$ vs. their filler content ϕ. The continuous curve plots the theoretical values of σ_{br} calculated, using the hypothesis of no adhesion between the two component phases, on the ground of the Nicolais–Narkis eq. (13).

References

1. J. A. Manson and L. H. Sperling, *Polymer Blends and Composites,* Plenum, New York, 1977, p. 373.

2. F. F. Lange, "Fracture and Fatigue" in *Composite Materials,* Vol. 5, L. J. Broutman, Ed., Academic, New York/London, 1974, p. 2.

3. (a) M. Vacatello and P. Corradini, *Gazz. Chim. Ital.,* **103,** 1027 (1973), (b) **104,** 773 (1974).

4. M. Vacatello, *Ann. Chim. (Rome),* **64,** 13 (1974).

5. M. Vacatello, *Ann. Chim. (Rome),* **64,** 19 (1974).

6. V. Busico, V. Salerno, and M. Vacatello, *Gazz. Chim. Ital.,* to appear.

7. E. Landi and M. Vacatello, *Thermoc. Acta,* **13,** 441 (1975).

8. E. Landi, V. Salerno, and M. Vacatello, *Gazz. Chim. Ital.,* **107,** 27 (1977).

9. M. Vacatello and P. Corradini, *Accad. Sci. Fis. Mat. (Naples),* **IV,** *XLIV,* 505 (1977).

10. C. Carfagna, M. Vacatello, and P. Corradini, *Gazz. Chim. Ital.,* **107,** 131 (1977).

11. M. R. Ciajolo, P. Corradini, and V. Pavone, *Gazz. Chim. Ital.,* **106,** 807 (1976).

12. G. C. Ives, J. A. Mead, and M. M. Riley, *Handbook of Plastic Test Methods,* Iliffe Books, 1971, p. 146.

13. L. Nicolais and M. Narkis, *Polym. Eng. Sci.,* **11,** 194 (1971).

14. A. Addeo, V. Busico, C. Migliaresi, and L. Nicolais, *Appl. Energy,* to appear.

Received October 24, 1979
Accepted March 25, 1980